Ecological Informatics 86 (2025) 103027

Contents lists available at ScienceDirect

Ecological Informatics

journal homepage: www.elsevier.com/locate/ecolinf

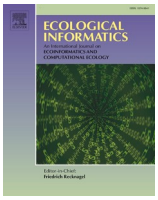

The construction of shelterbelts along the desert highway has increased the carbon sequestration capacity of the Taklimakan Desert, China

Ali Mamtimin [a,b,c,d,g,*], Kun Zhang [a,b,d,e], Hajigul Sayit [f], Yu Wang [a,b,c,d], JiaCheng Gao [a,b,c,d], Ailiyaer Aihaiti [a,b,c,d], Meiqi Song [a,b,c,d], Junjian Liu [a,b,c,d], Fan Yang [a,b,c,d], Chenglong Zhou [a,b,c,d], Wen Huo [a,b,c,d], Siqi Wang [a,b,d,e], Yangyao Xu [a,b,d,e], Gulinur Amar [a,b,c,d], Wei Liu [a,b,d,e]

[a] Institute of Desert Meteorology, China Meteorological Administration, Urumqi 830002, China
[b] National Observation and Research Station of Desert Meteorology, Taklimakan Desert of Xinjiang, Urumqi 830002, China
[c] Taklimakan Desert Meteorology Field Experiment Station of China Meteorological Administration, Urumqi 830002, China
[d] Xinjiang Key Laboratory of Desert Meteorology and Sandstorm, Urumqi 830002, China
[e] College of Geography and Remote Sensing Sciences, Xinjiang University, Urumqi 830046, China
[f] Xinjiang Meteorological Society, Urumqi 830002, China
[g] Tazhong Meteorological Station, Korla 841000, China

ARTICLE INFO

Keywords:
Desert highway
Shelterbelts
Taklimakan Desert
Carbon sequestration capacity

ABSTRACT

Human endeavors exert profound influences on the storage of carbon and the net primary productivity (NPP) of land, particularly in the environmentally sensitive arid territories. The Taklimakan Desert, known as the second largest migratory desert on Earth, necessitates an examination of the effects of the desert thoroughfare and its adjoining ecological windbreaks on carbon sequestration. This inquiry employed a myriad of data sources and harnessed the Integrated Valuation of Ecosystem Services and Trade-offs (InVEST), Carnegie-Ames-Stanford Approach (CASA), and Patch-level Land Use Simulation Model (PLUS) methodologies to delve into the spatial and temporal metamorphosis and future outlook of the Taklimakan Desert in China over the past three decades. The findings reveal that grasslands serve as the preeminent carbon reservoir in the Taklimakan Desert, witnessing a surge of 16.31 tons over the previous 30 years. Of particular note, the ecological windbreaks encircling the desert highway have bolstered carbon storage by an added 0.15 tons from the completion of the road in 1996 to 2020. Moreover, following the establishment of the ecological windbreak in 2005, there has been a notable upsurge in the values of net primary productivity (NPP) within this locality. Looking towards the future, various prospective scenarios, especially those centered on ecological conservation, underscore an escalating carbon sequestration effect in the Taklimakan Desert. Concurrently, there is an augmentation in carbon retention linked to the desert thoroughfare. The prognostications of maximum, minimum, and mean NPP values from 2030 to 2100 exhibit substantial oscillations, delineating the intricate interplay between climatic shifts and human endeavors in shaping regional NPP. In sum, these revelations intimate that well-designed human undertakings have engendered an expansion of verdant domains within the desert, ultimately benefiting carbon capture in these parched terrains.

1. Introduction

In the ethereal realm of terrestrial ecosystems, the process of carbon sequestration assumes a paramount role in governing the emission of greenhouse gases, notably carbon dioxide, into the ethereal expanse and in mitigating the ramifications of planetary climate metamorphosis (Piao et al., 2018). Against the backdrop of the strategic imperatives concerning the achievement of a "carbon peak" and the realization of "carbon neutrality", the intensification of inquiries into carbon sequestration within terrestrial ecosystems bears profound implications for the

* Corresponding author at: Institute of Desert Meteorology, China Meteorological Administration, Urumqi 830002, China.
E-mail address: ali@idm.cn (A. Mamtimin).

https://doi.org/10.1016/j.ecoinf.2025.103027
Received 6 September 2024; Received in revised form 15 January 2025; Accepted 15 January 2025
Available online 18 January 2025

global carbon vortex and the sustainable progression of ecosystems (Dabu and Xiaoxin, 2021; Dai Er et al., 2016; Solomon et al., 2013; Van Pham et al., 2023; Vendrame et al., 2018; Wei et al., 2011).

In contemporary times, a multitude of distinguished scholars, both nationally and internationally, have delved into the intricate realm of carbon sequestration and net primary productivity (NPP). While their investigations into carbon storage vary in scope, they can be categorized into three principal avenues: studies on the estimation of carbon storage, research on methods for estimating carbon storage, and inquiries into the spatiotemporal evolution mechanisms and influential factors shaping carbon storage (Shuchao et al., 2023; Verma et al., 2024; Xuejie et al., 2022; Yang et al., 2016; Yang Yuping and Wenmin, 2023; Zafar et al., 2024; Zhang et al., 2020; Zhang et al., 2023; Zhao et al., 2018). In the dawn of the 21st century, with the continuous enrichment of remote sensing observation data sensitive to land cover information and the rapid evolution of remote sensing processing technology(Zafar et al., 2023), a new era of land NPP estimation models has emerged. These models, which integrate remote sensing data, offer distinct advantages in capturing spatiotemporal heterogeneity. The recent advent of multi-scale and multi-resolution remote sensing data has further advanced our ability to quantify the intricate spatiotemporal characteristics of model parameters (Changqiao et al., 2017). Chen et al. (2022) conducted a study utilizing the sophisticated GeoSOS FLUS model to simulate the intricate spatial configuration of land use in the Daxing District. Shengtao et al. (2022) meticulously refined the conventional CASA model utilizing data sourced from the China Ecosystem Research Network (CERN).

These groundbreaking studies not only deepen our comprehension of ecosystem carbon cycling but also establish a scientific basis for addressing climate change and devising prudent land management and forest protection policies. With advancements in remote sensing technology and sophisticated model simulation techniques, forthcoming investigations are poised to achieve heightened precision and comprehensiveness. Deserts, as a crucial component of terrestrial ecosystems, are widely dispersed across global land, encompassing a total area of approximately 7 million square kilometers, constituting one-fourth of the Earth's land mass. In recent years, the issue of desertification has become increasingly salient amidst the escalating impacts of global climate change. China has sequentially implemented a series of national key ecological initiatives, such as the management of sand sources in the Beijing-Tianjin region, the conversion of farmlands into forests and grasslands, the Three-North Shelter Forest Program, and the holistic treatment of rocky desertification, facilitating a transformative shift from "encroaching sands and fleeing populations" to "advancing greenery and receding sands" (Fang et al., 2019; Mammitin, 2015; Wang and Huang, 2020; Zhang et al., 2009). The afforestation project aimed at carbon sequestration in the Kubuqi Desert region has effectively mitigated wind and sand hazards, enhanced the local ecological milieu, and accelerated both ecological development and the progression towards an ecological civilization (Qiao, 2022). It is evident that in the past, emphasis was predominantly placed on the outcomes of wind control, sand stabilization, microclimate amelioration, and economic enrichment following desertification mitigation, while the potential benefits of carbon sequestration were long overlooked (Ma et al., 2021; Yang et al., 2016).

The nexus between carbon sequestration in man-made shelterbelts in arid regions and NPP holds profound ecological and environmental management ramifications. In desert locales, plant proliferation is constrained by the availability of water and nutrients. Nevertheless, artificial shelterbelts have the capability to augment NPP in these regions through the introduction of drought-tolerant plant species and the implementation of efficient soil and water conservation practices. There exists a positive correlation between NPP and carbon sequestration; while NPP can serve as a rough indicator of carbon fixation rates, carbon storage embodies a protracted accumulation process with potential temporal lags between the two variables (Dan et al., 2023).The ecological endeavor of establishing a shelter forest along the Tarim Desert Highway stands as the longest desert shelter forest traversing a shifting desert worldwide, embodying a quintessential epitome of artificial desert ecosystems. Spanning approximately 446 km in length and 72 to 78 m in width, this shelterbelt serves as a protective shield for the desert highway. Through an exclusive focus on the shelter forest along the Taklimakan Desert Highway, this study delved into the carbon sequestration and spatio-temporal evolution characteristics of the Taklimakan Desert from 1990 to 2020 utilizing the InVEST model, alongside assessing the spatio-temporal evolution pattern of the NPP of the Taklimakan Desert employing the CASA model. Subsequently, through the utilization of land use type data, projections were made concerning the carbon sequestration and NPP of the Taklimakan Desert over the ensuing three decades.Through the aforementioned research endeavors, the influence of erecting artificial shelter forests in deserts on the intrinsic carbon sequestration capability of the desert was scrutinized, furnishing a scientific underpinning for the governance and advancement of desert ecosystems in response to climate fluctuations, while aspiring to provide a blueprint for the sustainable advancement and governance of desert ecosystems.

2. Materials and methods

2.1. Study area

The Taklimakan Desert, located within the coordinates of 36°50′ to 41°10′ N and 77°40′ to 88°20′ E, nestles at the core of the Tarim Basin, embraced by the grand Tianshan Mountains in the north and the formidable Kunlun Mountains in the south. Revered as the largest wandering desert in China and the second largest globally, it stretches across an impressive expanse of approximately 33.76×10^4 km^2. Residing within a temperate climate zone, it boasts an average annual temperature of 9–11 °C, a yearly precipitation rate of 11.05 mm, and an evaporation rate averaging at 3638.6 mm annually (Song et al., 2022).

The soil makeup is predominantly comprised of sandy particles, while flora is a scarce sight, restricted to species such as tamarisk, camel thorn, and thistle that somehow endure an existence in the sand dune valleys and on the peripheries of this hostile terrain. Encircling the desert are patches of verdant greenery, referred to as "sand sea green islands," teeming with abundant populations of Populus euphratica forests and tamarisk, as well as "green corridors" flanking the Hotan Riverbanks, vibrant with reeds and Populus euphratica flourishing.

Despite the formidable and inhospitable characteristics of the Taklimakan Desert, numerous crucial oases punctuate its periphery, strategically situated to harness the resources of local rivers and underground aquifers for sustenance. Prominent among these verdant sanctuaries are the Kashgar Oasis, Hotan Oasis, Korla Oasis, and Aksu Oasis, providing a refreshing contrast to the harsh desolation of their arid environs. The Taklimakan Desert boasts a network of meticulously engineered desert thoroughfares, notably including the Tarim Desert Road, completed with great care in 1995, extending over an impressive total length of 552 km. This road elegantly connects Korla City and Minfeng County, securing its place as the world's longest route cutting through undulating desert terrain. Another notable desert highway, stretching from Tazhong to Ruoqiang County, spans a grand distance of 436 km and was masterfully established in 2007. This road gracefully links the Tazhong Oilfield nestled deep within the heart of the Taklimakan Desert with Ruoqiang County. To combat the erosive forces of frequent sandstorms, imposing sand barriers and intricately designed grass grid sand barriers have been thoughtfully erected along the length of the highway. Moreover, hardy drought-resistant shrubs and lush herbaceous vegetation such as willow and poplar have been tenderly planted, forming a protective green embrace around the landscape. The Tarim Desert Highway features a standard roadbed width of approximately 11 m, with lane widths of 9 m and sturdy 1-m-wide shoulders on either side. The expanse of the verdant buffer zone adjusts according to

the topography and desert conditions, typically ranging from 50 to 100 m.

2.2. Datasets

The essential data required for this study encompasses the geospatial delimitations of provinces (Xu and Yang, 2022), the patterns and characteristics of land use (Jie et al., 2021), socio-economic indicators (Xu and Yang, 2022), climatic attributes (Musheng et al., 2018), and topographical features (Table 1). The boundaries defining administrative divisions are represented in vector format. (See Fig. 1.)

The analysis of land use dynamics and the consequent assessment of carbon sequestration capacity in response to these changes predominantly hinge upon data sourced from the China Land Cover Dataset (CLCD) meticulously curated by the esteemed team spearheaded by Professor Yang Jie and Professor Huang Xin at Wuhan University. This dataset, extracted from Landsat imagery accessible via the Google Earth Engine platform, encompasses a diverse array of 9 distinctive land cover classifications: arable expanses, sylvan realms, verdant shrubbery, pastoral grasslands, aqueous bodies, glacial ice and snowscapes, barren desolation, impermeable urban surfaces, and aqueous marshlands. For the purposes of this scholarly inquiry, land cover information spanning the years 1990, 2000, 2010, and 2020 was fastidiously curated and subsequently distilled into 6 overarching land cover categories: cultivated lands, forested domains, grassy expanses, aquatic enclaves, urbanized precincts, and fallow or untended terrains.

The data regarding drivers of change is harnessed to model the imminent shifts in land use. In this sphere, socio-economic influencers include indicators such as Gross Domestic Product (GDP), demographic figures, and spatial factors like proximity to urban hubs, transportation arteries, water bodies, and nodes of connectivity. Geospatial information encompasses digital elevation models (DEMs), slope characteristics, and aspect data, with a resolution down to 30 m.

Meteorological and ecological factors, including annual precipitation levels, temperature metrics, and soil composition data, have a profound impact on the environment. Precipitation and temperature data are crucial for accurately determining carbon density coefficients. Additionally, soil composition data is instrumental in predicting future land use trends.

Considering the fluctuations in spatial resolution of the aforementioned datasets and the vastness of the study region, we will standardize all data to a spatial resolution of 30 m.

Table 1
Data Types and Sources.

Types	Data	Resolution ratio	Data sources
Provincial administrative boundaries	Boundary of research area	vector data	Resource and Environmental Science and Data Center of Chinese Academy of Sciences (https://www.resdc.cn)
Land use data	CLCD	30 m	Wuhan University (doi: https://doi.org/10.5281/zenodo.5816591)
Socioeconomic factors	GDP	1 km	Resource and Environmental Science and Data Center of Chinese Academy of Sciences (https://www.resdc.cn)
	population	1 km	
	city	vector data	OpenStreetMap (https://www.openstreetmap.org/)
	road	vector data	
	water area	vector data	
	station	vector data	
Climate and environmental factors	precipitation	1 km	Resource and Environmental Science and Data Center of Chinese Academy of Sciences (https://www.resdc.cn)
	temperature	1 km	
	soil	1 km	
terrain data	DEM	30 m	Geospatial Data Cloud(http://www.gscloud.cn)
	slope	30 m	Obtained based on ArcGIS
	aspect	30 m	

2.3. Data processing methods

2.3.1. InVEST model

The InVEST model is applied for the spatialization and visualization of ecological service functions and economic values under different land cover scenarios. This study utilizes the carbon sequestration model in terrestrial ecosystems, calculating regional total carbon storage by multiplying four carbon reservoirs with various land use categories and aggregating the outcomes. The formula for calculation is as follows:

$$C_i = C_{above} + C_{below} + C_{soil} + C_{dead} \tag{1}$$

$$C_{total} = \sum_{i=1}^{n} C_i \times S_i \tag{2}$$

Where C_i is the total carbon density contained in the land use type ($t \cdot hm^{-2}$); C_{above}、C_{below}、C_{soil}、C_{dead} are respectively the above-ground carbon density, below-ground carbon density, soil carbon density, and dead organic matter carbon density ($t \cdot hm^{-2}$);C_{total} is the total carbon storage of the ecosystem (t); S_i is the area (hm^2) of land use type i; n is the number of land use types.

The information regarding the carbon density distribution among diverse land utilization classifications predominantly originates from the National Ecological Data Center Resource Sharing Service Platform (http://www.nesdc.org.cn/). Discrepancies may arise between the carbon density data associated with different land usage categories and the gathered dataset.A notable, positive correlation has been detected between biomass, soil organic carbon density, and precipitation, while a negative correlation is apparent with temperature. A sophisticated strategy that capitalizes on the intricate relationship between temperature and precipitation data to refine the initial carbon density statistics has been widely embraced in arid regions. Consequently, this methodology is implemented to refine the carbon density metrics concerning various land use categories within the research domain, ultimately providing accurate carbon density values for the study area (refer to Table 2). The specific procedural details are outlined as follows:

$$C_{sp} = 3.3968 \times MAP + 3996.1 \tag{3}$$

$$C_{BP} = 6.798 \times e^{0.0054 \times MAP} \tag{4}$$

$$C_{BT} = 28 \times MAT + 398 \tag{5}$$

$$K_{BP} = \frac{C_{BP}^{'}}{C_{BP}^{''}}\ K_{BT} = \frac{C_{BT}^{'}}{C_{BT}^{''}} \tag{6}$$

$$K_B = \frac{K_{BP}}{K_{BT}}\ K_s = \frac{C_{SP}^{'}}{C_{SP}^{''}} \tag{7}$$

Where C_{sp} is the soil carbon density corrected for annual precipitation; C_{Bp} is the biomass carbon density adjusted for annual precipitation; C_{BT} is the biomass carbon density adjusted for annual average temperature; MAP is the annual average precipitation (mm); MAT is the annual average temperature (°C). K_{BP} is the biomass carbon density precipitation correction coefficient; K_{BT} is the temperature correction coefficient for biomass carbon density; K_B is the biomass carbon density correction factor; K_S is the soil carbon density correction factor; C′ and C″ respectively represent the carbon density data of the Taklimakan Desert and the whole country.

2.3.2. CASA model

The net primary productivity (NPP) of vegetation epitomizes the

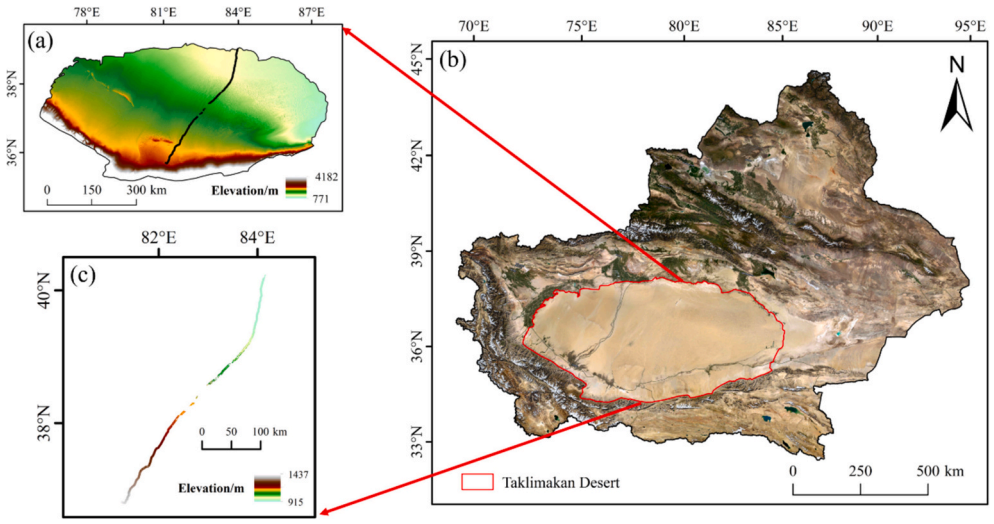

Fig. 1. Overview of the research area. (a) Xinjiang, China; (b) Taklimakan Desert; (c) Desert Highway.

Table 2
Carbon Density of Different Land Use Types in the Taklimakan Desert (Revised).

land-use type	Above-ground carbon density	Below-ground carbon density	Soil carbon density (0–100 cm)	Dead organic carbon density
Farmland	2.01	3.28	28.33	0
Forest	23.28	5.77	50.54	0
Grassland	0.44	3.56	38.24	0
Water	0.41	0.26	0	0
Built-up	0	0.17	34.06	0
Unused	0.29	0.24	0.69	0

cumulative organic matter amassed by verdant flora per unit area and time. Three classifications of models are employed to approximate NPP: statistical, parameter, and process-oriented. In this exploration, the esteemed CASA model (Xu and Yang, 2022), which computes NPP predicated on luminous energy utilization proficiency, was utilized. This model is notably well-suited for evaluating NPP on a regional scale.The requisite data inputs for the CASA model encompass temperature and precipitation records procured from the esteemed National Meteorological Science Data Center (https://data.cma.cn/), solar radiation statistics also acquired from the National Meteorological Science Data Center (https://data.cma.cn/), NDVI information extrapolated from the monthly peak composite NDVI product in China spanning from 1982 to 2020, and land and vegetation categorization details sourced from NASA's MCD12Q1 V006 dataset (https://modis.gsfc.nasa.gov/data/dataprod/mod12.php). This study leveraged USGS Landsat 9 Level 2 Collection 2 Tier 1 remote sensing imagery data and implemented the random forest technique for land classification, achieving a commendable overall accuracy quotient of 0.9. Furthermore, the CASA model was engaged in this examination to conduct minute-scale NPP simulations along the desert thoroughfares in southern Xinjiang, and meticulous land utilization categorization was orchestrated utilizing the sophisticated Google Earth Engine (GEE).The CASA model predominantly assesses the NPP of local foliage by taking into account two pivotal elements: the photosynthetically active radiation (APAR) absorbed by plants and the genuine luminous energy utilization efficiency (ε). The computational formula is delineated as follows:

$$\mathrm{APAR}(x,t) = \mathrm{SOL}(x,t) \times \mathrm{FPAR}(x,t) \times 0.5 \tag{8}$$

Where SOL(x,t) is the total solar radiation at position x at time t ($MJ{\cdot}m^{-2}{\cdot}month^{-1}$); FPAR($x$,$t$)refers to the proportion of vegetation's absorption of incident photosynthetically active radiation (PAR); 0.5 represents the proportion of solar effective radiation that vegetation can utilize to the total radiation.

The degree of solar radiation absorbed by vegetation is intricately linked to both the density of vegetative coverage and the unique botanical composition. Potter et al. proposed that the normalized vegetation index (NDVI), extracted from satellite-derived data, presents a dependable portrayal of vegetative canopy status, outlined in the subsequent equation:

$$FPAR(x,t) = \frac{FPAR(x,t)_{NDVI} + FPAR(x,t)_{SR}}{2} \tag{9}$$

$$FPAR(x,t)_{NDVI} = \frac{\left(NDVI(x,t) - NDV_{i,min}\right)}{\left(NDVI_{i,\mathrm{mux}} - NDVI_{i,min}\right)} \times FPAR_{max} - FPAR_{\min}\Big) + FPAR_{\min} \tag{10}$$

$$FPAR(x,t)_{SR} = \frac{\left(SR(x,t) - SR_{i,min}\right)}{\left(SR_{i,max} - SR_{i,min}\right)} \times \left(FPAR_{max} - FPAR_{\min}\right) + FPAR_{\min} \tag{11}$$

Where the values of SRi and min are 1.08, and the range of SRi and max is 4.14–6.17, Obtain SR (x, t):

$$SR(x,t) = \frac{[1 + NDVI(x,t)]}{[1 - NDVI(x,t)]} \tag{12}$$

2.3.3. PLUS model

The advanced model, referred to as the PLUS model, is deeply rooted in the delineation of established land typologies and utilizes raster data to forecast alterations at the patch level in land usage. This intricate model identifies instances of mutual transformations among varied classifications within land use datasets, subsequently producing forecasts of land utilization based on transition probabilities. The application of the random forest algorithm enables the calculation of expansion patterns and the identification of driving forces influencing each land category, thus providing insights into the growth potential of individual land classes and the impact exerted by diverse factors. Building upon the 2020 land use dataset as its fundamental basis, this study integrates a spectrum of distinct driving factors to simulate and predict changes in land use patterns up to the year 2050.

In the contemplation of future land utilization typology, three distinct narratives are intricately delineated: the organic progression, the conservation of ecology, and the advancement towards sustainability. The organic progression narrative serves as the fundamental storyline, wherein the gradual unfolding of natural development aligns with historical precedent, shaping the envisioned landscape

configuration at a measured pace. Conversely, the conservation of ecology narrative advocates for the strengthening of ecological habitats, imposing rigorous constraints on the transformation of wooded areas into alternative land uses, while allowing the conversion of grasslands solely into lush woodlands. The narrative of advancement towards sustainability highlights the intricate balance between economic progress and environmental protection, prescribing limits on the conversion of cultivable lands, woodlands, and aquatic realms.The detailed depiction of the financial implications of land use conversions across these multifaceted narratives is elegantly presented in Table 3, where a binary system of 1 indicating permissible conversions and 0 representing impermissible alterations is meticulously evaluated. (See Table 4.)

The evaluation of the PLUS model's simulation performance was conducted by measuring two metrics: overall accuracy (OA) and Kappa coefficient. The Kappa coefficient was computed according to the following formula:

$$Kappa = \frac{po - pc}{pp - pc} \tag{13}$$

where Kappa is the simulation accuracy index, *Po* is the actual simulation accuracy, *Pc* is the expected simulation accuracy under random conditions, and *Pp* is the simulation accuracy under ideal conditions. Generally, when the Kappa value is greater than 0.75, the simulation accuracy is high; a value between 0.4 and 0.75 means that the simulation accuracy is moderate; and when it is less than 0.4, the simulation accuracy is poor. The Kappa coefficient of the simulation accuracy in this study was 0.80, the OA was 0.92, and the simulation results met the research requirements.

2.3.4. Accuracy verification

As a result of the complexities involved in gathering observational data in the Southern Xinjiang region, this study conducted a comparative validation utilizing the NPP estimates derived from the Carnegie Ames Stanford Approach (CASA) model and the Moderate Resolution Imaging Spectroradiometer (MODIS). By randomly selecting 60 data points from each year's simulation results, a total of 240 valid data points were obtained. As depicted in Fig. 2, the precision validation results demonstrate an R^2 value of 0.698, indicating a strong correlation between the two datasets, thereby confirming the enhanced reliability of the NPP results simulated in this investigation.

Table 4
Land Use Type Area of Taklimakan Desert from 1990 to 2020.

Land-use type	Area/km^2			
	1990	2000	2010	2020
Farmland	2722.22	3277.12	4693.11	5794.81
Forest	3209.49	3269.68	3269.04	3239.29
Grassland	51,066.43	47,147.23	32,357.72	31,634.85
Water	1498.51	2021.97	1450.85	1485.29
Built-up	438.73	295.76	199.05	297.62
Unused	290,555.39	293,479.31	307,521.73	307,039.43

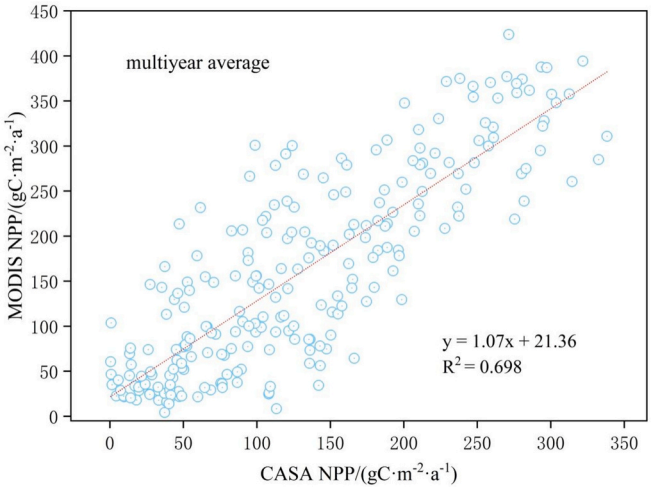

Fig. 2. Comparative Accuracy Validation of CASA NPP and MODIS NPP from 2000 to 2020.

3. Results

3.1. Land use transformation in the Taklimakan Desert over the previous three decade

The depiction in Fig. 3 unveils that throughout the past thirty years, the prevailing land utilization patterns within the Taklimakan Desert have predominantly been desolate, encompassing roughly 88 % of the total land area under scrutiny. Subsequent to barren lands, grasslands,

Table 3
Cost matrix of land use conversion in multi-scenario simulation.

Land use scenario	Type	Farmland	Forest	Grassland	Water	Built-up	Unused
Natural development scenario	Farmland	1	1	1	1	1	1
	Forest	1	1	1	1	1	1
	Grassland	1	1	1	1	1	1
	Water	1	1	1	1	1	1
	Built-up	1	1	1	1	1	1
	Unused	1	1	1	1	1	1
Ecological protection scenario	Farmland	1	1	1	1	1	0
	Forest	0	1	0	0	0	0
	Grassland	0	1	1	0	0	0
	Water	0	0	0	1	0	0
	Built-up	1	1	1	1	1	0
	Unused	1	1	1	1	0	1
Sustainable development scenario	Farmland	1	0	0	0	1	0
	Forest	0	1	0	0	0	0
	Grassland	1	1	1	1	1	0
	Water	0	0	0	1	0	0
	Built-up	0	1	1	1	1	0
	Unused	1	1	1	1	1	1

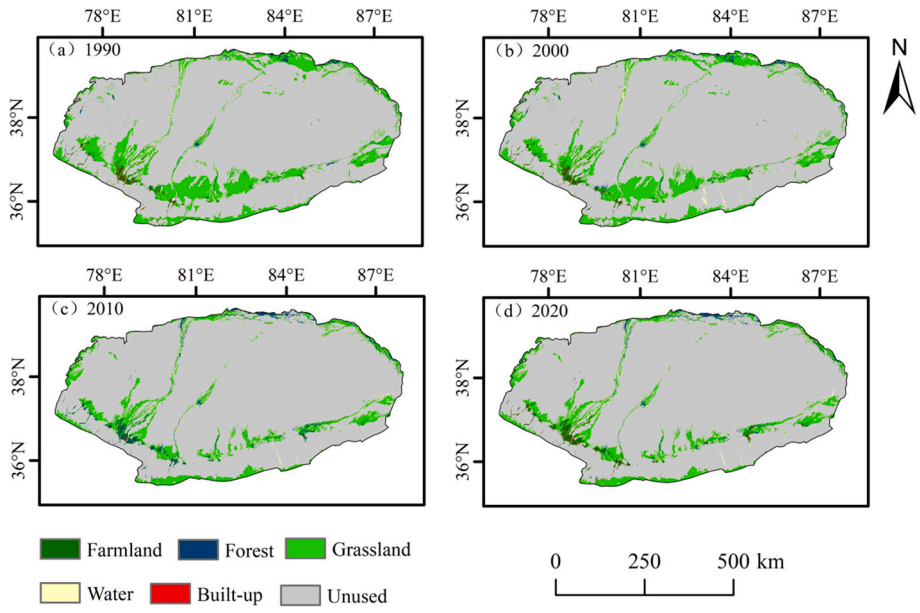

Fig. 3. Spatial and Temporal Distribution in Land Use in the Taklimakan Desert from 1990 to 2020.

farmlands, forests, water bodies, and urban areas constitute the rest of the scenery. Significantly, the allocation of wooded regions varies between the two zones, with forests mainly clustered along the southern and northern peripheries of the Taklimakan Desert, as well as in the proximity of the desert highway. (See Fig. 4.)

Moreover, a scrutiny of the evolutionary trends in the spatial and temporal distribution patterns of land utilization unveils captivating revelations. Particularly, the Taklimakan Desert experienced a remarkable upsurge in cultivable land extent from 1990 to 2020, marking a substantial enlargement of 3072.59 km^2. The most notable escalation transpired between 2000 and 2010, encompassing roughly 46 % of the collective expansion in arable land. Closely trailing behind is the amplification in wooded regions, amounting to 29.8 km^2.

Fascinatingly, the course of land apportionment for developmental endeavors unveils an undulating trajectory, initially marking a descent of 239.68 km^2 from 1990 to 2010, succeeded by an escalation of 98.57 km^2 from 2010 to 2020. Concerning aqueous expanses, their kinetics manifest a rhythmic sequence of augmentation, diminution, and subsequent augmentation once more. Notably, the epoch spanning from 1900 to 2000 witnessed an increment of 523.46 km^2, counteracted by a downturn of 571.12 km^2 between 2000 and 2010, only to revive with an augmentation of 34.44 km^2 between 2010 and 2020.

In sharp juxtaposition, grasslands are undergoing an enduring decrease, with a significant diminishing of 19,431.6 km^2 from 1990 to 2020. On the contrary, wastelands are on an ascending path, observing ceaseless expansion totaling 16,484.04 km^2 between 1990 and 2020.

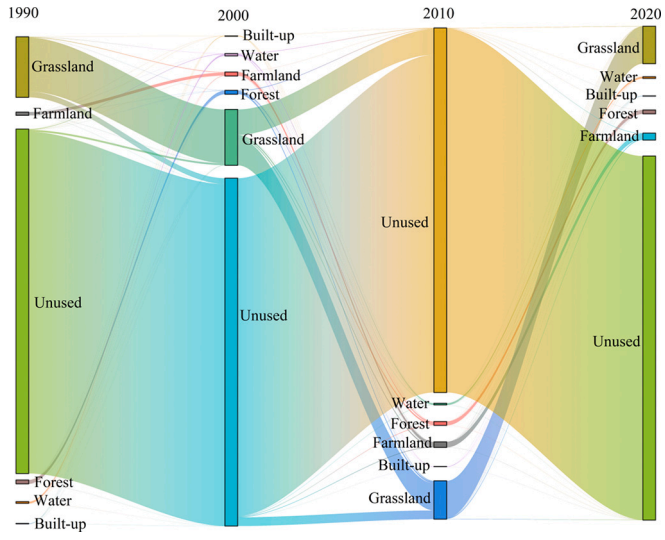

Fig. 4. Sankey Map of Land Use Changes in the Taklimakan Desert from 1990 to 2020.

3.2. *Spatial and temporal fluctuations in carbon storage in the Taklimakan Desert from 1990 to 2020 utilizing the InVEST model*

The assessment of carbon sequestration in the Taklimakan Desert ecosystem using the InVEST model spanning from 1990 to 2020 unveils a consistently ascending trajectory since the inception of observations (See Figs. 5, 6). Of particular note is the pinnacle of carbon storage reached in 2020, standing at an impressive 133.33 tons, with 2010 in close pursuit at 129.9 tons, and 2000 trailing at 123.49 tons. The initial measurement in 1990 documented the most modest figure of 109.66 tons, indicating a notable surge of 23.67 tons over the course of three decades. (See Fig. 7.)

The distribution of carbon sequestration among different land use categories within the Taklimakan Desert showcases a diverse range, from minor to significant contributions. These categories encompass meadows, fallow lands, croplands, urban areas, woodlands, and water bodies. Throughout the observed timeframe spanning from 1990 to 2020, the total carbon storage within the Taklimakan Desert has consistently increased. Notably, the meadows emerge as a crucial reservoir within the desert, experiencing a gradual rise from 58.30 tons in 1990 to 74.61 tons in 2020, reflecting a substantial gain of 16.31 tons over the span of three decades. In contrast, the fallow lands (deserts) represent the second-largest carbon repository, yet undergo an annual decrease, dropping from 40.71 tons in 1990 to 39.94 tons in 2020, indicating a decline of 0.77 tons within the same timeframe (Table 5). (See Table 6.)

The transformation of carbon sequestration across diverse land use categories experiences subtle fluctuations over distinct epochs. Throughout the observational period spanning from 1990 to 2020, carbon sequestration within grasslands, cultivated lands, and urban areas demonstrates an upward trajectory, while undeveloped territories show a slight decrease. Cultivated lands have surged from 10.57 tons in

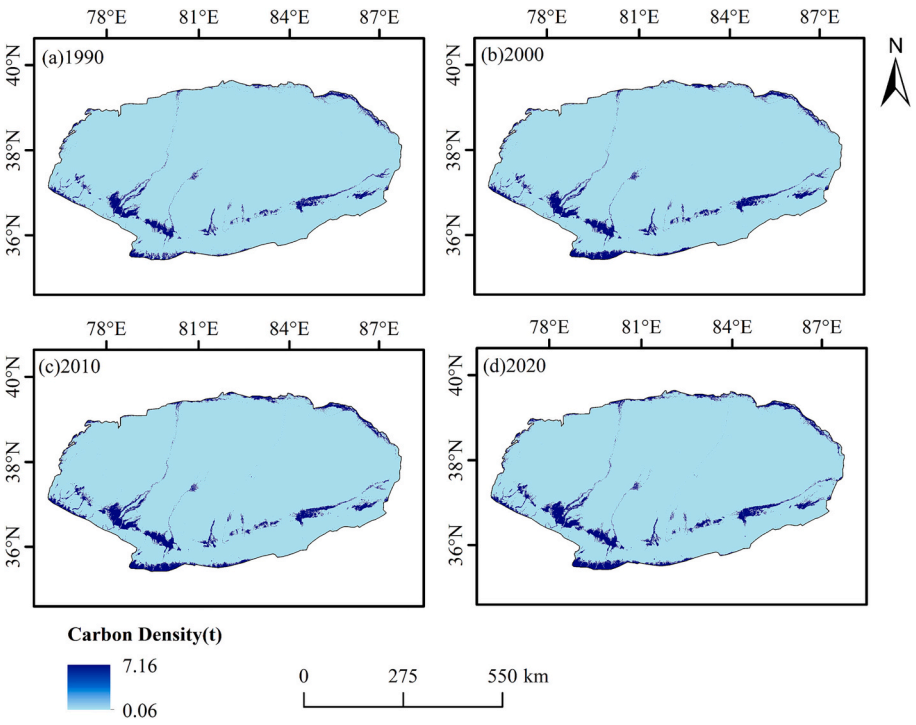

Fig. 5. Current Status of Carbon Storage in the Taklimakan Desert from 1990 to 2020.

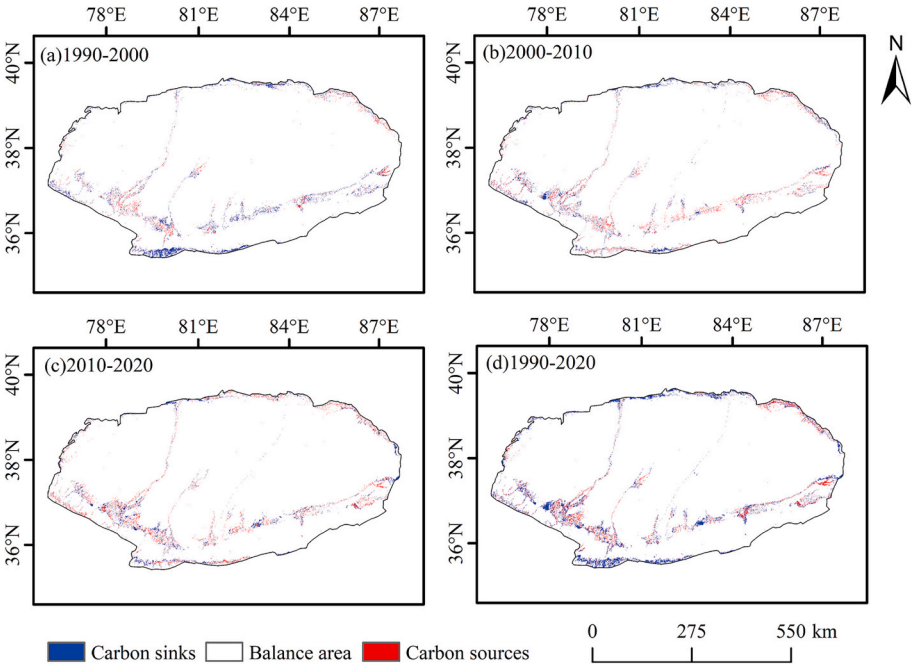

Fig. 6. Changes in Carbon Storage in the Taklimakan Desert from 1990 to 2020.

1990 to 17.75 tons in 2020, displaying a consistent upward trend; simultaneously, grasslands have experienced substantial growth from 58.3 tons in 1990 to 74.61 tons in 2020, resulting in a net increase of 16.31 tons over three decades. Of particular note is their dominance, comprising 55.96 % of the total carbon sequestration in the Taklimakan Desert. Forested landscapes and aquatic expanses remain relatively stable; in contrast, undeveloped lands have seen a decline from 40.71 tons in 1990 to 39.94 tons in 2020, indicating a marginal decrease of 0.77 tons over the past 30 years, yet maintaining a significant 29.96 % share of the overall carbon sequestration.

Moreover, the carbon sequestration within the lands utilized by desert highways remains relatively low. From 1990 to 2020, the carbon storage in cultivated lands, grasslands, and urban areas showed an increasing trend, while the unused lands saw a decrease. After the construction of the desert highway, carbon storage increased from 0.66 tons in 2000 to 0.71 tons in 2020, representing an improvement of 0.16 tons over almost two decades. The building of desert highways has led to a reduction in unused lands (deserts), resulting in a decrease in carbon storage from 0.193 tons in 2000 to 0.183 tons in 2020, indicating a decrease of 0.01 tons over approximately two decades. Therefore,

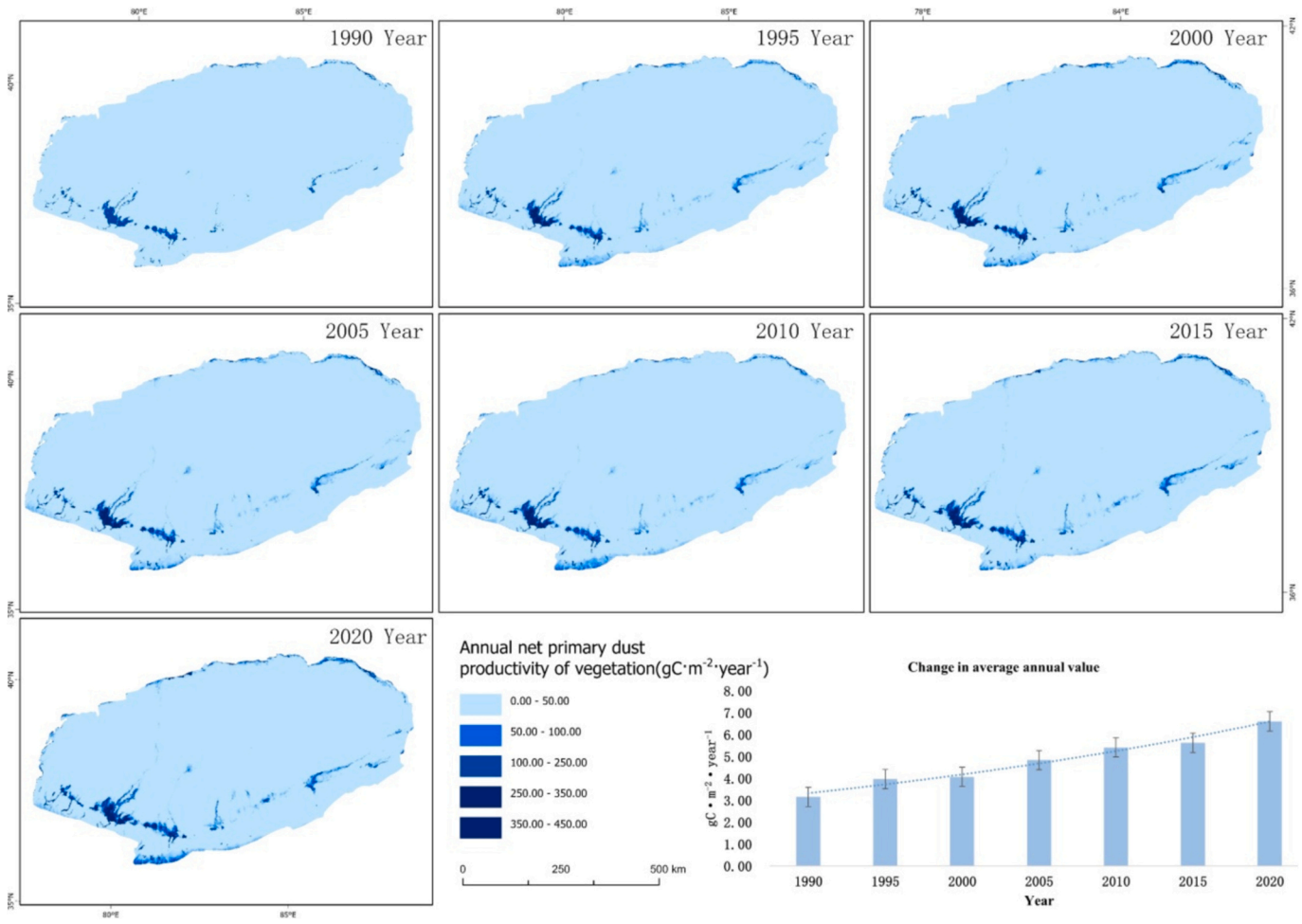

Fig. 7. Spatial Changes of NPP in Southern Xinjiang over the Past 30 Years.

Table 5
Carbon Storage of Various Land Use Types in the Taklimakan Desert from 1990 to 2020.

LUCC	Carbon storage / t			
	1990	2000	2010	2020
Farmland	10.57	12.16	14.81	17.75
Forest	0.01	0.01	0.01	0.01
Grassland	58.30	70.81	74.56	74.61
Water	0.01	0.01	0.01	0.01
Built-up	0.06	0.21	0.43	1.01
Unused	40.71	40.29	40.08	39.94

Table 6
Carbon Storage of Various Land Use Types in Desert Highways from 1990 to 2020.

LUCC	Carbon storage / t			
	1990	2000	2010	2020
Farmland	0.04	0.13	0.15	0.21
Grassland	0.58	0.66	0.74	0.71
Built-up	0.0002	0.001	0.007	0.014
Unused	0.193	0.188	0.184	0.183

following the completion of the desert highway in 1996, the ecological shelterbelts near the desert highway have increased their carbon storage by 0.15 tons by 2020.

From a spatial distribution perspective, the Taklimakan Desert showcases significant variability in carbon storage levels, with heightened concentrations primarily located in the southern, southeastern, southwestern, and northeastern sectors, while lower concentrations are evident in the central and northern regions. Spatial variation analysis unveils distinct zones within the desert ecosystem: a zone emitting carbon, a zone of balance, and a zone absorbing carbon. The zone of balance, characterized by values ranging from −0.1 to 0.1 metric tons, denotes areas where carbon storage remains relatively stable. Fig. 6 demonstrates that carbon storage levels remained largely constant across most regions from 1990 to 2020, indicating a state of equilibrium. Nevertheless, between 2000 and 2020, there was a noticeable surge in carbon absorption areas, particularly in the southern, southeastern, and southwestern regions.

3.3. Temporal and spatial fluctuations of net primary productivity in the enigmatic Taklimakan Desert from 1990 to 2020 using the CASA model

As an indispensable ecological barrier in China, the preservation and sustainable development of the ecological environment in the southern region of Xinjiang have always been of paramount concern. The construction of the Taklimakan Desert Highway in 1995 has had a profound and enduring impact on the regional ecological landscape, thanks to years of painstaking efforts in building ecological protection forests.To delve deeper into the specific effects of ecological protection forest construction on NPP in southern Xinjiang, this study utilized advanced USGS Landsat 9 Level 2 Collection 2 Tier 1 remote sensing imagery data. The random forest method was employed for land classification, achieving an impressive overall accuracy rate of 90 %. Furthermore, the

CASA model was utilized in this research to conduct small-scale NPP simulations along the desert highways in southern Xinjiang, while refined land use classification was carried out using the sophisticated Google Earth Engine (GEE) platform.

By closely examining the variations in NPP in the southern region of Xinjiang, the critical role of ecological protection forests in improving the local ecological environment has been revealed. The results of this analysis indicate that since the completion of the highway in 1995, especially after the establishment of ecological protection forests in 2005, there has been a significant rise in NPP in southern Xinjiang. This suggests that the ecological protection forests along the desert highway not only increase the vegetation cover in the area, but also enhance the productivity and resilience of the overall ecosystem. Through continuous efforts in building ecological protection forests, the ecological landscape in southern Xinjiang has seen remarkable improvements, providing valuable scientific foundations and practical insights for future ecological conservation and sustainable development initiatives.

Analyzing the data covering the years 1990 to 2020 reveals a consistent increase in the annual NPP in the southern region of Xinjiang. Upon careful examination of the findings presented in Table 7, it becomes evident that following the construction of the Taklimakan Desert Highway in 1995, there was a significant rise in the NPP levels, particularly after the establishment of the ecological protection forest in 2005. During this period, the NPP value surged from 0.467 in 1995 to 0.825 in 2010. Although experiencing a slight decline to 0.748 in 2020, the NPP remains substantially elevated compared to the early stages of road development.The spatial distribution of NPP in southern Xinjiang from 1990 to 2000 exhibited a modest yet relatively uniform distribution, indicating sparse vegetation cover and limited ecosystem productivity in the region. From 2000 to 2010, there was a gradual increase in the NPP levels, predominantly concentrated along the highways, underscoring the significant impact of the ecological protection forest on the local ecosystem. Progressing from 2010 to 2020, despite a continued upward trend in NPP values, the growth rate slowed down, possibly due to the reinforcement of ecological conservation measures implemented throughout the highway corridor.

3.4. Changes in carbon storage in the Taklimakan Desert under various future scenarios

By leveraging the land utilization data projected by the sophisticated PLUS model and amalgamating it with the InVEST model, the computation of carbon sequestration in the Taklimakan Desert for the year 2050 across diverse scenarios – encompassing natural progression, ecological preservation, and sustainable advancement – offers profound insights into the prospective condition of this distinctive ecosystem (refer to Fig.8). The spatial apportionment of carbon sequestration in 2050 exhibits a relatively congruent distribution to that of 2020, delineating a discernible ring-shaped configuration enveloping the north, south, southwest, and northeast sectors. The central vast expanse, defined by its arid terrain, stands in stark contrast to the urban and rural expansions that encircle it. Significantly, the execution of ecological engineering endeavors, notably the establishment of ecological shelterbelts alongside desert thoroughfares, has engendered a substantial augmentation in carbon sequestration within the vicinity.

Table 7
Changes in NPP in Southern Xinjiang over the Past 30 Years.

Year	Maximum value	Minimum value	Average value
1990	279.85	0.15	3.16
1995	345.97	0.14	3.98
2000	323.61	0.14	4.08
2005	391.46	0.28	4.85
2010	430.90	0.15	5.42
2015	433.52	0.16	5.63
2020	426.99	0.15	6.61

Fig. 9 elegantly depicts the evolution of carbon sequestration in the majestic expanse of the Taklimakan Desert over the temporal span from 2020 to 2050. Manifestly, a discernible ascent in the levels of carbon storage is observed, gracefully surpassing the achievements of the preceding decade (refer to Fig. 9 for a visual representation). Within the realm of organic progression, regions witnessing an elevation in carbon sequestration predominantly cluster in the southwestern quadrant, albeit accompanied by subtle undulations. Conversely, the transformative influence of ecological preservation strategies manifests palpably as carbon sequestration experiences a remarkable upsurge when juxtaposed against both natural and sustainable developmental scenarios. This surge can be attributed to the stringent protocols governing land utilization within ecologically safeguarded zones, mandating the conversion of grasslands into verdant arboreal expanses. Consequently, the proliferation of wooded domains has precipitated a substantial augmentation in carbon sequestration capacities. Within the paradigm of sustainable development, the incremental shifts mirror those documented within the natural developmental framework.

3.5. Spatiotemporal dynamics of net primary productivity in the Taklimakan Desert under various future scenarios

The NPP stands as a crucial measure in evaluating the vitality of ecosystems, representing the total organic carbon produced by plants through photosynthesis minus the carbon released through plant respiration. Fluctuations in NPP have profound impacts on the flow of carbon within ecosystems and the intricate web of global climate patterns. The southern regions of Xinjiang are situated in arid and semi-arid zones, where NPP is influenced by both natural climate variations and human activities. Exploring the nuances of NPP in southern Xinjiang within a forward-looking framework provides valuable insights into how ecosystems respond to changes in climate, thus forming a solid foundation for developing effective ecological protection measures and management strategies. Utilizing data from the advanced CMIP6 scenario and the respected CASA model, we conducted simulations to analyze the trajectory of NPP in southern Xinjiang from 2030 to 2050. By examining the maximum, minimum, and average NPP values over different time periods, the fluctuations in NPP become evident. Table 8 outlines the peak, lowest, and average NPP values in southern Xinjiang throughout the period from 2030 to 2050. In the broader context, the highest NPP values display noticeable fluctuations from year to year, while the lowest NPP values show a degree of consistency across the entire timeframe, with variations staying within a narrower range. At the same time, the average NPP values exhibit a rising and falling trend, indicating a favorable environment for plant growth. Adequate rainfall and optimal temperatures contribute to increasing the efficiency of photosynthesis in plants, leading to higher NPP levels.The spatial distribution of NPP in southern Xinjiang from 2030 to 2050, illustrated in Fig. 10, reveals a certain level of uniformity with occasional fluctuations over different time periods. Areas with higher NPP are predominantly found in oases and along river corridors in southern Xinjiang, contrasting with regions of lower NPP that are prevalent in dry desert expanses.

4. Discussion

4.1. Influencing factors of carbon storage in the Taklimakan Desert

This research employed the InVEST model to evaluate the spatial allocation of carbon sequestration in the Taklimakan Desert of Xinjiang from 1990 to 2050. The study uncovered notable fluctuations in carbon storage within the Taklimakan Desert. Starting from the year 2000, the carbon storage escalated from 0.66 tons to 0.71 tons by the year 2020. Despite the desert highways construction diminishing the expanse of unused land (desert), consequently leading to a decline in corresponding carbon storage, the diverse vegetation in the ecological shelterbelts flanking both sides of the highway has amplified carbon storage through

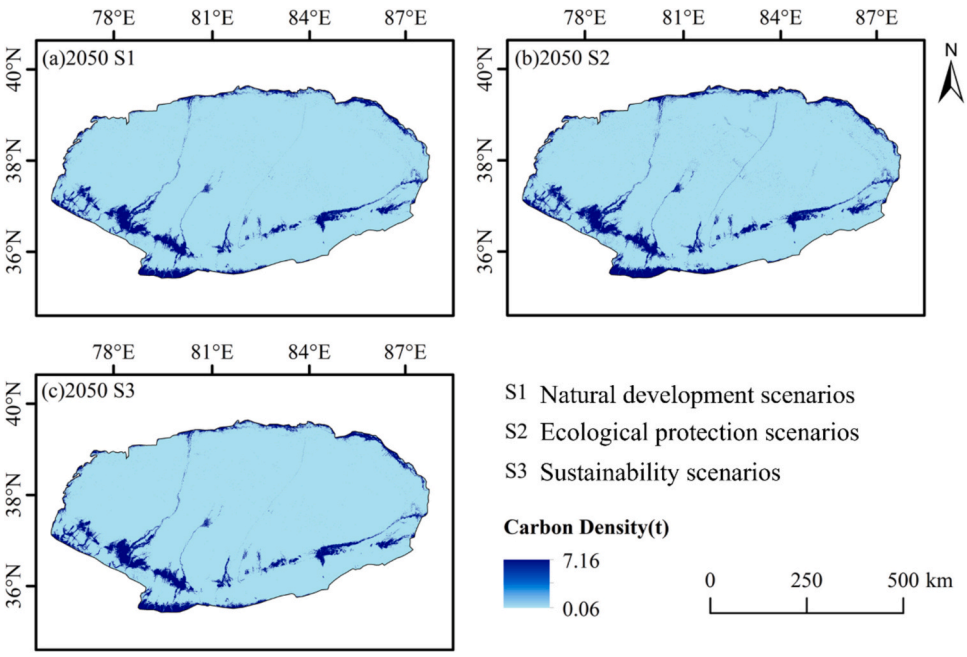

Fig. 8. Current Status of Carbon Storage in the Taklimakan Desert in 2050 under Various Scenarios.

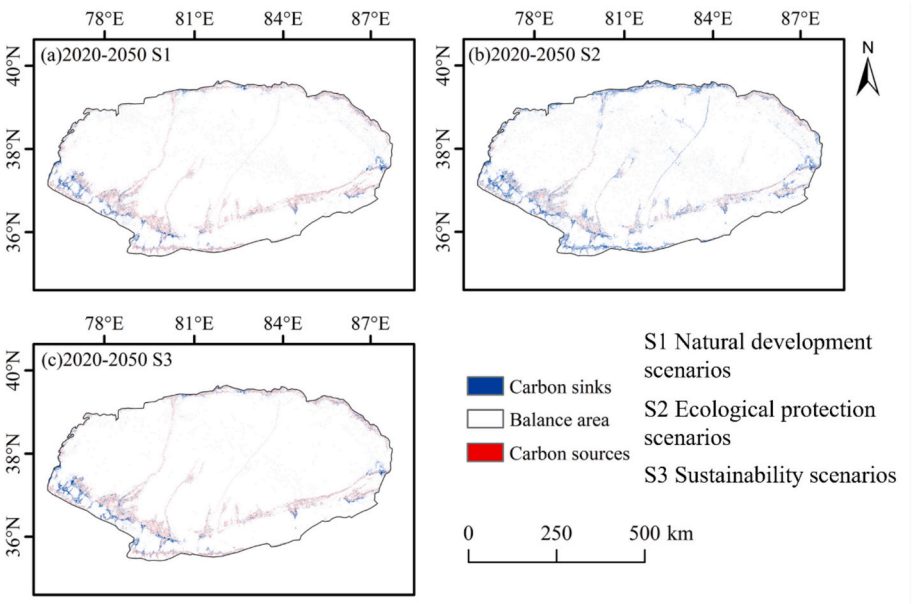

Fig. 9. Changes in carbon storage in the Taklimakan Desert under various scenarios from 2020 to 2050.

Table 8
Changes in NPP in Southern Xinjiang under future scenarios.

Year	Maximum value	Minimum value	Average value
2030	692.75	0.18	8.58
2040	675.45	0.19	8.44
2050	671.27	0.20	8.75

the mechanisms of photosynthesis and other biological processes. Overall, following the completion of the desert highway in 1996, the carbon storage in the ecological shelterbelts surrounding the highway escalated by 0.15 tons by 2020.

Spatially, the regions with high carbon storage in the Taklimakan Desert are predominantly situated at the southern and northern perimeters of the desert, whereas regions with lower values are mainly concentrated in the heart of the desert and alongside the highway. The rationale behind the high-value regions lies in the existence of continuous and sporadic grasslands, farmland, as well as a modest quantity of forest and water bodies, with grasslands representing the most widespread vegetative cover.

From a chronological standpoint, between 1990 and 2020, carbon storage burgeoned from 10.57 tons in 1990 to 17.75 tons in 2020, registering a cumulative augmentation of 7.18 tons, propelled by the consistent expansion of arable land. Despite the gradual reduction in grassland area over nearly three decades, totaling a decrease of 19,431.6Km^2, carbon storage paradoxically surged by 16.31 tons. Within the realm of the desert highway segment, the carbon storage of agricultural and construction lands steadily climbed from 1990 to 2020,

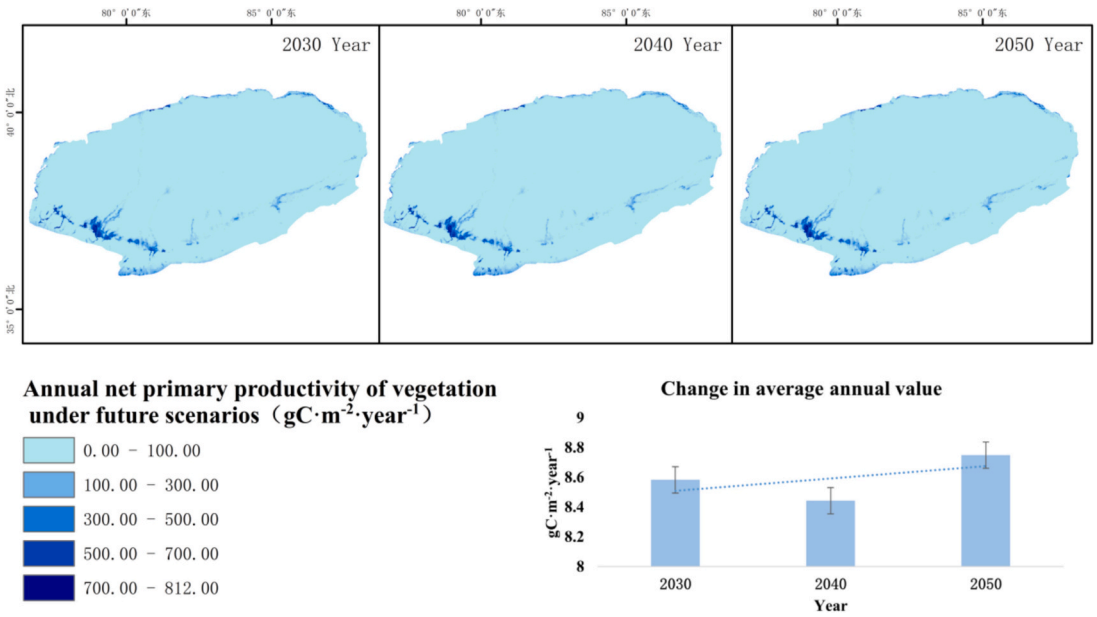

Fig. 10. Changes in net primary productivity of vegetation in the Taklimakan Desert under future scenarios from 2030 to 2050.

while the carbon storage of grasslands initially soared and subsequently dwindled, yet overall witnessed an increase of 0.13 tons. Conversely, the unused land exhibited a progressive diminishing trend over time.

Moreover, by utilizing land use data prognosticated by the PLUS model and integrating it with the InVEST model, the carbon storage of the Taklimakan Desert in 2050 was projected under three scenario models. The spatial distribution patterns in these three scenarios exhibited minimal deviations when juxtaposed with the year 2020. Nevertheless, in the S2 scenario, the fortification of the ecological shelterbelts along the desert highway markedly elevated its carbon storage capacity.

Changes in land use patterns have a significant impact on carbon storage levels (Tianqi et al., 2022; Zafar et al., 2024), as evidenced by the proliferation of verdant expanses in the deserts of southern Xinjiang and the comprehensive integration of lush vegetation along desert thoroughfares. These transformations have initiated substantial shifts in land utilization within the expansive Taklimakan Desert. The spatial organization of carbon sequestration exhibits a certain level of unpredictability, with a diverse trend emerging after the year 2000, aligning with numerous scholarly investigations both domestically and internationally (Can et al., 2023; Xinyan et al., 2024). For instance, in their examination of land use dynamics in the Poyang Lake Basin, Liu and colleagues determined that the sprawling urban development is the primary driver of carbon loss in the region (Musheng et al., 2018). Yang and team utilized a blend of the CA Markov model and the InVEST model to analyze the cumulative effects of various land use changes across six distinct time periods on ecosystem carbon storage in the Yellow River Basin. Their research revealed a decline in ecosystem carbon sequestration due to shifts in land use, particularly in swiftly urbanizing areas, with a projected decrease of 258.863 million metric tons by the year 2030 when compared to 2018 levels (Yang et al., 2022). Zhao et al. (2018) embarked on an extensive examination of land use transformations and their impact on carbon sequestration in the upper reaches of the semi-arid northwest Heihe River Basin over the next 15 years, utilizing sophisticated cellular automata models and InVEST models. Their results revealed a promising trend in carbon retention within the upper reaches, attributed to efforts in ecological restoration, with a cumulative increase of 10.27 Tg from 2015 to 2029. Conversely, regions not subject to ecological interventions experienced a decrease in carbon storage.

Adelisardou et al. (2022) conducted a comprehensive analysis of the intricate relationships between historical land use changes from 2000 to 2019 and projected scenarios from 2019 to 2046 on carbon sequestration in the Girot Plain of Iran, employing a blend of GEE, cellular automata models, and InVEST models. Their research identified a sharp decline in carbon storage associated with the expansion of agricultural activities and rapid urbanization, resulting in an annual loss of −475,547 Mg/year in carbon sequestration in the plain. Indeed, the modification of land utilization patterns resulting in carbon emissions exerts a deleterious effect on the sequestration of carbon in ecological systems. The Intergovernmental Panel on Climate Change has recognized the impact of land use transformation on carbon retention within the broader framework of land use modifications (Kanglong et al., 2022; Loukika et al., 2023; Shujun, 2023; Yang Yuping and Wenmin, 2023; Yi Dan and Minghao, 2022; Zhang et al., 2023). Hence, it is vital to implement corresponding ecological preservation strategies, actively advocate for the establishment of ecological infrastructure, diminish the overall anthropogenic alterations in land use, and thus augment the holistic capacity of ecosystems to sequester carbon.

4.2. *Influencing factors of NPP in the Taklimakan Desert*

In recent decades, the amalgamation of shifting meteorological patterns and anthropogenic activities has etched a profound imprint on the local ecosystem and botanical vigor (Krivoguz, 2024). Through our sophisticated prognostications employing the state-of-the-art CASA model within the visionary CMIP6 future projection, the NPP in southern Xinjiang is on the brink of undergoing remarkable metamorphoses from 2030 to 2100, with both the peak and mean values reaching their zenith in the promising year of 2060. This trajectory impeccably mirrors the ambitious national targets delineated by China, aspiring to cap carbon emissions prior to 2030 and achieve carbon neutrality by the momentous milestone of 2060 (Li et al., 2023).

In a prospective scenario, the heightened precipitation and optimal temperatures create ideal conditions for the process of photosynthesis in plants, significantly boosting its efficiency. Expanding upon prior research, our simulation also unveils significant regional variations in the spatial distribution patterns of NPP, with areas of high value predominantly clustered in verdant oases and fertile river valleys, where ample water resources nourish plant life with vital nutrients. Conversely, regions of low value are primarily situated in arid desert landscapes, where the scarcity of water severely inhibits plant growth,

leading to decreased NPP (Li et al., 2016). The allocation of water resources is acknowledged as a critical factor influencing NPP, as sufficient water supply not only stimulates plant growth but also enhances overall ecological productivity within a specific region. Furthermore, our study identifies the construction of the Taklimakan Desert Highway and the implementation of protective afforestation as pivotal factors contributing to the increase of NPP in southern Xinjiang.

Since the commencement of the ecological protection forest project in 1995, there has been a notable upsurge in the regional NPP metric. Of particular significance is the era following 2005, during which the annual average NPP metric soared from 0.467 in 1995 to 0.825 by 2010. This revelation stands as a testament to the effectiveness of the ecological protection forest project in the Taklimakan Desert, not only in enhancing vegetation coverage but also in enriching the productivity and resilience of the ecosystem (Chen et al., 2017). Our investigation represents a groundbreaking endeavor in examining the variations in NPP subsequent to the establishment of the desert highway in southern Xinjiang. Prior to this, there had been a scarcity of similar studies, particularly in terms of outlining the trajectories and specific temporal points of NPP fluctuations in prospective scenarios (Ge et al., 2021; Teng et al., 2020). These findings underscore the crucial role of ecological engineering interventions in improving the regional ecological landscape, promoting botanical growth, and enhancing the overall functionality of the ecosystem, thereby providing strong support for ecological conservation and sustainable development in southern Xinjiang.

4.3. Potential applications and limitations

In this investigation, the primary methodologies employed encompass the sophisticated InVEST, CASA, and PLUS frameworks. The InVEST model functions by analyzing land usage metrics in conjunction with carbon density statistics, wherein said carbon density metrics are meticulously fine-tuned using temperature and precipitation data specific to the research locale, thereby conferring a nuanced degree of localized relevancy. The CASA model intricately computes NPP subsequent to parameter refinements predicated on the region-specific dataset, thereby ensuring a discernible benchmark of operational aptness. Meanwhile, the dynamic PLUS model engenders simulations rooted in historical land utilization patterns within the study domain, thus proffering expansive heuristic utility.

Nevertheless, these models are not without constraints. One noteworthy limitation pertains to the InVEST model, specifically in relation to its reliance on historical data to estimate carbon density. Given the ongoing impact of human activities on the natural landscape, the dynamic nature of carbon density necessitates real-time adjustments for more precise simulations of carbon storage. Consequently, forthcoming research endeavors should integrate field measurements of carbon density within the study locale to uphold the veracity of analytical outcomes.

5. Conclusion

Utilizing an array of diverse data sources, the InVEST and CASA models were harnessed to scrutinize the spatial and temporal distribution patterns of carbon storage and NPP within the Taklimakan Desert throughout the previous three decades. This examination entailed a meticulous evaluation of the alterations in carbon storage and NPP induced by the installation of the desert highway. Additionally, through the integration of the PLUS model with CMIP6 climate models, we explored the prospective trajectories of carbon storage and NPP in the Taklimakan Desert across a spectrum of scenarios.

The discoveries unveil that the grasslands function as the principal carbon reservoir in the Taklimakan Desert, having undergone a surge of 16.31 tons during the preceding three decades. Furthermore, subsequent to the development of the desert thoroughfare in 1996, the ecologically beneficial shelterbelts encircling the highway have enriched the carbon repository by an additional 0.15 tons by the year 2020. Particularly noteworthy is the marked elevation in NPP indices across southern Xinjiang subsequent to the establishment of the ecological shelterbelt in 2005.

As we gaze into the future through various lenses, particularly those that prioritize the preservation of our precious ecosystems, the phenomenon of carbon sequestration in the majestic Taklimakan Desert emerges with ever greater clarity. This results in a corresponding augmentation of carbon storage along the desert highway, painting a vivid picture of the potential impact of ecological protection efforts.

Projections indicate that the peak values for both maximum and average NPP are anticipated to manifest in the year 2060, hinting at the presence of favorable climatic conditions during this time under the various future scenarios considered. These findings collectively highlight the profound and constructive influence of eco-conscious initiatives on the intricate carbon dynamics within this parched expanse.

CRediT authorship contribution statement

Ali Mamtimin: Writing – review & editing, Project administration, Funding acquisition, Formal analysis, Data curation. **Kun Zhang:** Writing – original draft, Data curation, Conceptualization. **Hajigul Sayit:** Software, Resources, Project administration, Methodology, Data curation. **Yu Wang:** Methodology, Investigation, Conceptualization. **JiaCheng Gao:** Software, Resources, Project administration, Methodology, Conceptualization. **Ailiyaer Aihaiti:** Validation, Software, Project administration, Conceptualization. **Meiqi Song:** Visualization, Supervision, Resources. **Junjian Liu:** Resources, Methodology. **Fan Yang:** Software, Methodology, Formal analysis, Conceptualization. **Chenglong Zhou:** Validation, Software, Project administration. **Wen Huo:** Visualization, Conceptualization. **Siqi Wang:** Resources, Investigation. **Yangyao Xu:** Resources, Project administration, Conceptualization. **Gulinur Amar:** Visualization, Validation, Software, Conceptualization. **Wei Liu:** Resources, Software.

Declaration of competing interest

The authors declare that they have no known competing financial interests or personal relationships that could have appeared to influence the work reported in this paper.

Acknowledgements

This study was supported by the “Tianshan Talent” Training Program - Science and Technology Innovation Team (Tianshan Innovation Team) Project (2022TSYCTD0007), National Natural Science Foundation of China (42305132, 42375084), Youth Innovation Team of China Meteorological Administration (CAM2024QN13), the Xinjiang Key Laboratory of Desert Meteorology and Sandstorms Award Funding: Grant number: 2023-38.

Data availability

All data of the research are available for download from the link (https://chogo.teracloud.jp/share/1261056419908ce9 or https://github.com/yangchuan/SupplementData.git).

References

Adelisardou, F., Zhao, W., Chow, R., Mederly, P., et al., 2022. Spatiotemporal change detection of carbon storage and sequestration in an arid ecosystem by integrating Google Earth engine and InVEST (the Jiroft plain, Iran). Int. J. Environ. Sci. Technol. 19 (7), 5929–5944. https://doi.org/10.1007/s13762-021-03676-6.

Can, Cai, Min, Fan, Jing, Yao, Lele, Zhou, Yuanzhe, Wang, Xiaoying, Liang, Liu, Zhaoqiang, Chen, Shu, 2023. Spatial-temporal characteristics of carbon emissions corrected by socioeconomic driving factors under land use changes in

Sichuan Province, southwestern China. Ecol. Indic. 77, 102164. https://doi.org/10.1016/j.ecoinf.2023.102164.
Changqiao, Hong, Xiaobin, Jin, Changchun, Chen, et al., 2017. A review of research on land net primary productivity estimation models integrating remote sensing data. Progress Geograph. Sci. 36 (8), 16. https://doi.org/10.18306/dlkxjz.2017.08.002.
Chen, X., He, X., Wang, S., 2022. Simulated validation and prediction of land use under multiple scenarios in Daxing district, Beijing, China, based on GeoSOS-FLUS model. Sustainability 14, 11428. https://doi.org/10.3390/su141811428.
Chen, Tiantian, Li, Peng, Dingde, Xu, et al., 2017. Spatio-temporal pattern of net primary productivity in Hengduan Mountains area, China: impacts of climate change and human activities. Chin. Geogr. Sci. 27 (6), 948–962.
Dabu, Jiang, Xiaoxin, Wang, 2021. Interpretation of drought change in IPCC sixth assessment report. J. Atmos. Sci. 44 (5), 650–653.
Dai Er, Fu, Huang, Yu, Zhuo, Wu, et al., 2016. Spatial and temporal patterns of carbon sources/sinks in grassland ecosystems in Inner Mongolia and their relationship with climate factors. J. Geogr. 71 (01), 21–34.
Dan, Luo, Zhongfa, Zhou, Quan, Chen, et al., 2023. The response of carbon storage in karst areas to land use patterns: a case study of the Nanbei Panjiang River Basin. J. Ecol. 43 (9), 3500–3516.
Fang, Xiao, Xiao, Li, Chengsen, Li, et al., 2019. Understanding the Taklimakan Desert. Life World 02, 52–53.
Ge, Wenyan, Deng, Liqiang, Wang, Fei, et al., 2021. Quantifying the contributions of human activities and climate change to vegetation net primary productivity dynamics in China from 2001 to 2016. Sci. Total Environ. 773, 145648. https://doi.org/10.1016/j.scitotenv.2021.145648.
Jie, Yang, Baopeng, Xie, Degang, Zhang, 2021. Research on spatiotemporal changes of carbon storage in the Yellow River Basin based on InVEST and CA Markov models. Chin. J. Ecol. Agric. (Chin. English). https://doi.org/10.13930/j.cnki.cjea.200746.
Kanglong, Deng, Qianqian, Wang, Xinyue, Chen, et al., 2022. Research progress and prospects of carbon emissions from land use. Green Technol. 09, 024.
Krivoguz, Denis, 2024. Geo-spatial analysis of urbanization and environmental changes with deep neural networks: insights from a three-decade study in Kerch peninsula. Ecol. Indic. 80 (102513), 1574–9541. https://doi.org/10.1016/j.ecoinf.2024.102513.
Li, Qing, Zhang, Chunlai, Shen, Yaping, et al., 2016. Quantitative assessment of the relative roles of climate change and human activities in desertification processes on the Qinghai-Tibet Plateau based on net primary productivity. Catena 147, 789–796. https://doi.org/10.1016/j.catena.2016.09.005.
Li, Lü, Wang, Shijie, Chen, Youping, et al., 2023. Climate change in the eastern Xinjiang of China and its connection to northwestern warm humidification. Atmosphere 14 (9), 1421.
Loukika, Kotapati Narayana, Keesara, Venkata Reddy, Buri, Eswar Sai, Sridhar, Venkataramana, 2023. Future prediction of scenario based land use land cover (LU&LC) using DynaCLUE model for a river basin. Ecol. Indic. 102223, 1574–9541. https://doi.org/10.1016/j.ecoinf.2023.102223.
Ma, Q., Wang, X., Chen, F., Wei, L., Zhang, D.K., Jin, H., 2021. Carbon sequestration of sand-fixing plantation of Haloxylon ammodendron in Shiyang River basin: storage, rate and potential. Glob. Ecol. Conserv. 28, e01607. https://doi.org/10.1016/j.gecco.2021.e01607.
Mammitin, Ali, 2015. Research on Carbon Budget Characteristics and Influencing Factors in Xinjiang Desert Region. Nanjing University of Information Science and Technology.
Musheng, Liu, Bangyou, Yan, Fang, Yu, 2018. Etc research on land use dynamic changes in Poyang Lake Basin based on GIS. Jiangxi Sci. 36 (1), 7. https://doi.org/10.13990/j.issn1001-3679.2018.01.013.
Piao, S., Meng, T., Zhuo, L., et al., 2018. Lower land-use emissions responsible for increased net land carbon sink during the slow warming period. Nat. Geosci. 11. https://doi.org/10.1038/s41561-018-0204-7.
Qiao, F., 2022. Practice on carbon sequestration measurement and monitoring of the carbon sequestration afforestation project in the Kubuqi Desert area—taking the carbon sequestration afforestation project of Inner Mongolia Yitai Group in Hangjin Banner as an example. Inner Mongolia Forestry Investig. Design 45 (04), 55–58.
Shengtao, Su, Yuan, Zeng, Dan, Zhao, et al., 2022. Optimization and analysis of estimation model for net primary productivity of land vegetation in China: based on China ecosystem research network data. J. Ecol. 42 (4), 14. https://doi.org/10.5846/stxb202011263031.
Shuchao, Gao, Yiqing, Chen, Zongzhu, Chen, et al., 2023. Carbon storage and spatial distribution characteristics of forest ecosystems in Hainan Island. J. Ecol. 43 (9), 3558–3570.
Shujun, Xu, 2023. Research on carbon emission effects and characteristics based on land use. Rural Sci. Exp. 6, 34–36.
Solomon, S., Pierrehumbert, R.T., Matthews, D., et al., 2013. Atmospheric composition, irreversible climate change, and mitigation policy. Environ. Sci. https://doi.org/10.1007/978-94-007-6692-1-15.
Song, Y., Chen, X., Li, Y., Fan, Y., Adrian, L. Collins., 2022. Quantifying the provenance of dune sediments in the Taklimakan Desert using machine learning, multidimensional scaling and sediment source fingerprinting. CATENA 210, 105902. https://doi.org/10.1016/j.catena.2021.105902.
Teng, Mingjun, Zeng, Lixiong, Wenjie, Hu, et al., 2020. The impacts of climate changes and human activities on net primary productivity vary across an ecotone zone in Northwest China. Sci. Total Environ. 714, 136691. https://doi.org/10.1016/j.scitotenv.2020.136691.
Tianqi, Rong, Pengyan, Zhang, Huiru, Zhu, Ling, Jiang, Yanyan, Li, Zhenyu, Liu, 2022. Spatial correlation evolution and prediction scenario of land use carbon emissions in China. Ecol. Inform. 71, 101802. https://doi.org/10.1016/j.ecoinf.2022.101802.
Van Pham, T., Do, T.A.T., Tran, H.D., 2023. A.N.T. Do assessing the impact of ecological security and forest fire susceptibility on carbon stocks in Bo trach district, Quang Binh province, Vietnam. Ecol. Inform. 74, 101962. https://doi.org/10.1016/j.ecoinf.2022.101962.
Vendrame, N., Tezza, L., Pitacco, A., 2018. Study of the carbon budget of a temperate-climate vineyard: inter-annual variability of CO_2 flux. Am. J. Enol. Vitic. 70 (1), 34–41. https://doi.org/10.5344/ajev.2018.18006.
Verma, Pragati, Siddiqui, Azizur Rahman, Mourya, Nitesh Kumar, et al., 2024. Forest carbon sequestration mapping and economic quantification infusing MLPnn-Markov chain and InVEST carbon model in Askot Wildlife Sanctuary, Western Himalaya. Ecol. Inform. 79 (102428). https://doi.org/10.1016/j.ecoinf.2023.102428.
Wang, S.Q., Huang, Y., 2020. Determinants of soil organic carbon sequestration and its contribution to ecosystem carbon sinks of planted forests. Glob. Chang. Biol. 26 (5), 3163–3173. https://doi.org/10.1111/gcb.15036.
Wei, Bai, Genxu, Wang, Guangsheng, Liu, 2011. Response of CO2 emissions during the growth period of alpine meadows on the Qinghai Tibet Plateau to temperature rise. Ecol. J. 30 (06), 1045–1051.
Xinyan, Wu, Caiting, Shen, Linna, Shi, Yuanyuan, Wan, Jinmei, Ding, Qi, Wen, 2024. Spatio-temporal evolution characteristics and simulation prediction of carbon storage: A case study in Sanjiangyuan Area, China. Ecol. Inform. 80, 102485. https://doi.org/10.1016/j.ecoinf.2024.102485.
Xu, Y., Yang, Y., 2022. A 5 km resolution dataset of monthly NDVI product of China (1982–2020), p. CSD 7. https://doi.org/10.11922/11-6035.csd.2021.0041.zh.
Xuejie, Bai, Xufeng, Wang, Xiaohui, Liu, Xuqiang, Zhou, 2022. Characteristics and driving factors analysis of carbon flux changes in wetland, farmland, and grassland ecosystems in the Heihe River Basin. Remote Sens. Technol. Appl. 37 (01), 94–107.
Yang Yuping, Hu, Wenmin, Jia Guanyu, et al., 2023. Scenario simulation of land use carbon storage in the Dongting Lake area based on InVEST and ANN-CA models. J. Nanjing For. Univ. (Nat. Sci. Ed.) 47 (4), 175–184. https://doi.org/10.12302/j.issn.1000-2006.202110020.
Yang, Y., Wang, G.X., Ran, F., et al., 2016. Litter carbon stock and spatial patterns of main forest types in Tibet. Chin. J. Ecol. https://doi.org/10.13292/j.1000-4890.201603.018.
Yang, F., et al., 2022. Evaluation of carbon sink in the Taklimakan Desert based on correction of abnormal negative CO_2 flux of IRGASON. Sci. Total Environ. 838, 155988. https://doi.org/10.1016/j.scitotenv.2022.155988.
Yi Dan, Ou, Minghao, Guo Jie, 2022. Etc research progress and trend prospects on carbon emissions and low-carbon optimization of land use. Resource Sci. 44 (8), 15. https://doi.org/10.18402/resci.2022.08.02.
Zafar, Z., Sajid Mehmood, M., Shiyan, Z., Zubair, M., Sajjad, M., Yaochen, Q., 2023. Fostering deep learning approaches to evaluate the impact of urbanization on vegetation and future prospects. Ecol. Indic. 146, 109788. https://doi.org/10.1016/j.ecolind.2022.109788.
Zafar, Zeeshan, Zubair, Muhammad, Zha, Yuanyuan, Mehmood, Muhammad Sajid, Rehman, Adnanul, Fahd, Shah, Nadeem, Adeel Ahmad, 2024. Predictive modeling of regional carbon storage dynamics in response to land use/land cover changes: an InVEST-based analysis. Ecol. Indic. 82, 102701. https://doi.org/10.1016/j.ecoinf.2024.102701.
Zhang, Z., Li, X., Liu, L., Jia, R., Zhang, J., Wang, T., 2009. Distribution, biomass, and dynamics of roots in a revegetated stand of Caragana korshinskiiin the Tengger Desert, northwestern China, 122 (1), 109–119. https://doi.org/10.1007/s10265-008-0196-2.
Zhang, Q., Lei, H., Yang, D., et al., 2020. Decadal variation of CO_2 flux and its budget in a wheat and maize rotation cropland over the North China Plain. Biogeosciences 17 (8), 2245–2262. https://doi.org/10.5194/bg-17-2245-2020.
Zhang, S., Hao, X.M., Zhao, Z.Y., et al., 2023. Natural vegetation succession under climate change and the combined effects on net primary productivity. Earth's Future. https://doi.org/10.1029/2023EF003903.
Zhao, M., He, Z., Du, J., et al., 2018. Assessing the effects of ecological engineering on carbon storage by linking the CA-Markov and InVEST models. Ecol. Indic. 98 (Mar), 29–38. https://doi.org/10.1016/j.ecolind.2018.10.052.